

Holding and Spinning Molecules in Space

Simon S. Viftrup,¹ Vinod Kumarappan,² Sebastian Trippel,³ and Henrik Stapelfeldt^{2,4}

¹*Department of Physics and Astronomy, University of Aarhus, DK 8000 Aarhus C, Denmark*

²*Department of Chemistry, University of Aarhus, DK-8000 Aarhus C, Denmark*

³*Physics Institute, University of Freiburg, D-79104 Freiburg, Germany*

⁴*Interdisciplinary Nanoscience Center (iNANO), University of Aarhus, DK-8000 Aarhus C, Denmark*

Edward Hamilton and Tamar Seideman

Department of Chemistry, Northwestern University, 2145 Sheridan Road, Evanston, Illinois 60208-3113, USA

(Received 9 May 2007; published 5 October 2007)

We illustrate, experimentally and theoretically, a laser-based method to control the rotations of polyatomic molecules in 3D space. A linearly polarized nanosecond pulse strongly aligns the most polarizable axis of an asymmetric top molecule along its polarization axis while an orthogonally polarized, femtosecond pulse sets the molecules into controlled rotation about the aligned axis. As a result, strong three-dimensional (3D) alignment occurs shortly after the femtosecond pulse and is repeated periodically, reflecting coherent revolution about the molecular axis. Our method opens new directions for research in orientationally confined complex molecules.

DOI: [10.1103/PhysRevLett.99.143602](https://doi.org/10.1103/PhysRevLett.99.143602)

PACS numbers: 42.50.Hz, 33.15.Bh, 33.80.-b, 42.65.Re

The alignment of molecules influences essentially all bimolecular and photochemical reactivity. As such, development and application of alignment techniques has been a topic of substantial importance and activity in molecular sciences for decades [1,2]. A significant advance of the field was made in the mid 1990s, when it was realized that moderately intense electromagnetic fields from pulsed lasers can align molecules along axes fixed in space [3,4]. Alignment results from the interaction between the (permanent or induced) electric dipole moment and the laser field and is very general, applying to any molecules (other than spherical tops) [5,6]. The rapid progress in laser induced alignment techniques over the past ten years has broadened the scope of spatially oriented molecules from the original focus on chemical reaction dynamics to new applications such as ultrafast electron or x-ray imaging [7–9], extreme nonlinear optics [10,11], and fs time-resolved photoelectron spectroscopy [12]. The vast majority of studies to date have focussed on linear molecules, but the growing range of applications of alignment in complex molecular systems is currently shifting attention to the nonlinear polyatomic domain, where complete control over the rotational motions requires one to go beyond alignment. In the limit of micron-sized particles, this task has already been accomplished by optical tweezer type techniques which allow mesoscopic objects to be held and rotated about any axis of choice [13]. Here we introduce a method, based on the combination of nanosecond and femtosecond laser pulses, that represents a step toward achieving this goal for molecules and illustrate its potential experimentally and theoretically. We use 3,5 difluoroiodobenzene (DFIB) molecules as a model but the approach is general.

Our method uses two linearly polarized laser pulses, one long and one short with respect to the molecular rotational

periods. The long pulse tightly aligns the most polarizable molecular axis along its polarization vector. Thereby, the interaction between this molecular axis and the orthogonally polarized short pulse is essentially eliminated. Instead, the short pulse interacts with the second most polarizable axis, which sets the molecule into coherent revolution about the arrested molecular axis. Quantum mechanically, the combined laser fields excite a coherent superposition of helicity levels that subsequently exhibits a revival pattern at a period characterizing the field-free rotational motion. This approaches a molecular version of an asymmetric rigid rotor spinning around an axis held fixed in space.

The numerical and experimental methods were described previously [5,14,15]. Briefly, a pulsed molecular beam, formed by supersonically expanding a gas mixture of a few mbar DFIB and 90 bar helium into vacuum [15], is crossed at 90° by three pulsed laser beams. The short alignment pulses [$\tau_{\text{short}} = 150$ fs (FWHM)] are electronically synchronized to the peak of the long alignment pulses ($\tau_{\text{long}} = 10$ ns). The probe pulses (30 fs, 3×10^{14} W/cm²), sent at a controllable delay, t , with respect to the short pulses, remove several electrons from the molecules, thereby triggering Coulomb explosion into ionic fragments. In particular, I⁺ and F⁺ fragment ions are useful experimental observables since they recoil along the symmetry axis and in the plane of the molecule, respectively. By recording the velocities of both ion species with 2-dimensional ion imaging (implemented by accelerating the ions with a weak static field towards a 2-dimensional detector), we determine the instantaneous molecular orientation at the time of the probe pulse [15].

Our numerical results are based on nonperturbative solution of the time dependent Schrödinger equation subject to the induced dipole interaction with the two laser fields.

Expansion of the rotational wave packet in a symmetric top representation results in a set of coupled differential equations for the expansion coefficients, where both the field-free (asymmetric top) and the field-induced coupling matrix elements are analytically soluble. Knowledge of the expansion coefficients (hence, of the complete system wave packet) as a function of time allows us to generate all observables for given sets of initial conditions. Finite temperature is accounted for through Boltzmann averaging of the initial-state-resolved observables.

We refer our results to two systems of axes: the one fixed in the laboratory and the other in the molecular frame—see Fig. 1(d). The space-fixed x and y axes are defined as the short and the long pulse polarization directions, respectively. The molecule-fixed Z axis is defined by the C-I bond axis, and the body-fixed X axis lies in the molecular plane.

We start by illustrating the sharp alignment of the most polarizable molecular axis (the C-I bond axis for the example of DFIB molecules) induced by the long pulse. To that end we compare I^+ images recorded with and without the long pulse. In the absence of the long pulse, the I^+ image is circularly symmetric [Fig. 2 (A1)] due to the cylindrical symmetry introduced by polarizing the probe pulse perpendicular to the detector plane. When the long pulse is applied, the I^+ ions exhibit strong angular localization about the polarization axis, as shown in the horizontal panel of Fig. 1(a), indicating that the molecules are adiabatically aligned [15]. Therefore, images taken with the long pulse polarization in the detector plane can

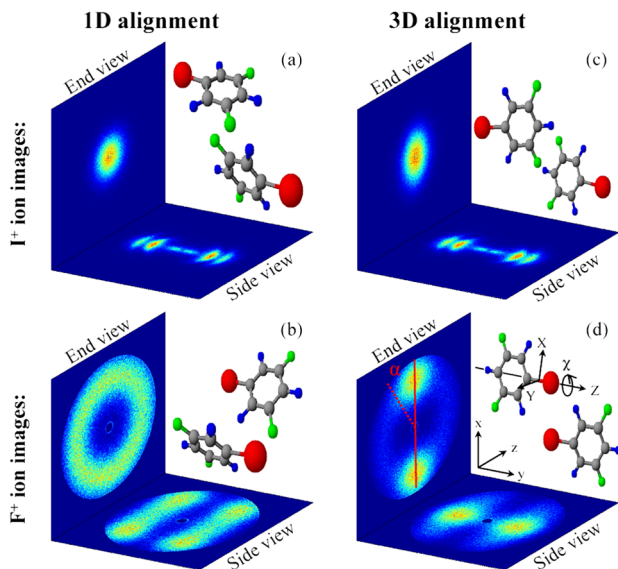


FIG. 1 (color online). Illustration of the correspondence between the observed ion images and the spatial orientation of the DFIB molecules. End views (vertical panels) are obtained by polarizing the long pulse perpendicular to the detector plane and side views (horizontal panels) by polarizing the long pulse parallel to the detector plane. (d) shows the laboratory-fixed (x, y, z) and molecule (X, Y, Z) coordinate systems as well as two of the angles (χ, α) used to describe the alignment—see text.

be regarded as a “side view” of the molecule. Similarly, images taken with the long pulse polarized perpendicular to the detector plane show “end views” of the molecule. The vertical panel of Fig. 1(a) shows the I^+ end view with the long pulse present. The tight confinement of the ions near the center [compared to the I^+ distribution without the long pulse, Fig. 2 (B1)] is an alternative way to visualize the 1D alignment.

Turning to the F^+ ions [vertical panel in Fig. 1(b), corresponding to an end view], we observe a perfect circularly symmetric ring structure, showing that the rotation of the molecular plane about the C-I axis is uniform. Combining the information from the I^+ and F^+ images, we conclude that the long pulse strongly aligns the C-I axis along the long pulse polarization but leaves the rotation about the C-I axis unrestricted.

Next, we investigate the effect on the molecular orientation when the short pulse is added. The end view of the F^+ ions shows a dramatic change at early times after the short pulse. Within the first three picoseconds, the initial circular symmetry is replaced by sharp localization along x —the short pulse polarization [Fig. 2 (D2)–(D4)], corresponding to alignment of the molecular plane parallel to the x, y plane [Fig. 1(d)]. In the end view of the I^+ ions it is seen that the initial circular distribution [Fig. 2 (B2)] develops into an elliptical shape at $t = 3$ ps [Fig. 2 (B4)], indicating that the C-I axis has suffered a minor distortion along the x axis, remaining, however, tightly confined [16]. Thus, strong alignment of both the C-I axis and the molecular plane, i.e., 3D alignment, occurs 3 ps after the short pulse. At later times the confinement of the F^+ in the end view is lost and at $t = 8$ ps [Fig. 2 (D5)] the circularly symmetric shape is restored, followed by mild confinement along the z axis at $t = 10$ ps [Fig. 2 (D6)]. This evolution from alignment to antialignment of the plane is more striking in the F^+ side view. Here planar

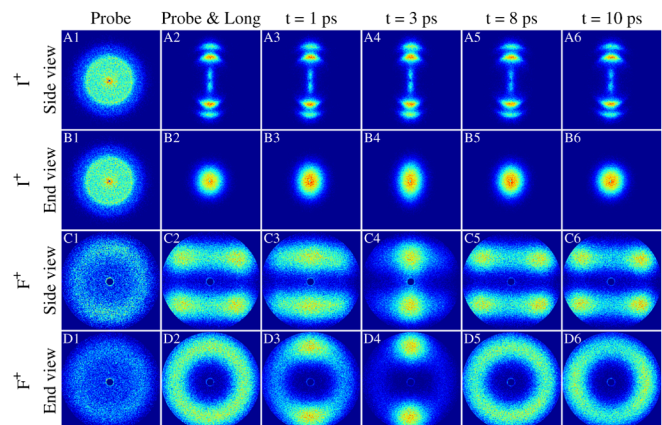


FIG. 2 (color online). Ion images of I^+ and F^+ fragments recorded in both end and side views. Column 1 (probe only) and 2 (probe and long pulse) serve as reference images. Column 3–6, recorded at different times after the short pulse, illustrate the alignment dynamics (see text). $I_{\text{long}} = 7 \times 10^{11}$ W/cm² and $I_{\text{short}} = 2 \times 10^{13}$ W/cm².

alignment at 3 ps manifests itself as two localized areas centered along the y axis [Fig. 2 (C4)]. The antialignment confines the molecular plane to the detector plane (y, z) and produces a four-center F^+ image [Fig. 2 (C6)]. This illustrates one of the advantages of the present method, regarded as a route to 3D alignment, over the use of a single elliptically polarized long pulse [17], where the 3D confinement is bound to occur in the polarization plane.

Proceeding to explore the possibility of observing reconstruction of the initial alignment of the molecular plane at much longer times, akin to the rotational revivals observed in 1D alignment [6], we repeated the measurements for times out to 450 ps. The results derived from F^+ end view images are summarized in Fig. 3, which shows the time evolution of $\langle \cos^2 \alpha \rangle$, where α is the angle between the projection of the F^+ ion velocity vector on the detector plane and the short pulse polarization vector [Fig. 1(d)]. At the strong planar alignment maximum, $t = 3$ ps, $\langle \cos^2 \alpha \rangle = 0.73$, whereas at the point of antialignment, $t = 10$ ps, it decreases to 0.47. Subsequently, $\langle \cos^2 \alpha \rangle$ is essentially flat with a value of 0.50 except for four transients centered at 74 ps, 146 ps, 217 ps, and 288 ps. At the strongest transient ($t = 146$ ps), where $\langle \cos^2 \alpha \rangle$ reaches a maximum value of 0.53, the initial planar alignment is restored although with reduced strength. End view images of the I^+ ions in the time interval around this transient are essentially indistinguishable from those obtained without the short pulse; i.e., the long pulse keeps the C-I axis strongly confined. We conclude that 3D alignment exhibits revivals, although with much weaker planar confinement than the maximum at 3 ps.

Further analysis of the positions of the transients shows that the transients at 3, 146, and 288 ps, which have similar shapes, are repeated periodically with a separation of ~ 143 ps. Noting the rotational constants of DFIB, $A = 1750$ MHz, $B = 484$ MHz, $C = 379$ MHz, we find that the observed period is essentially $1/(4A) = 143$ ps. This value has the significance of the period for a full rotation of the molecular plane about the symmetry axis, corresponding to A -type revivals using the terminology of rotational coherence spectroscopy [18]. The positions of the weak transients observed between the major transients classify

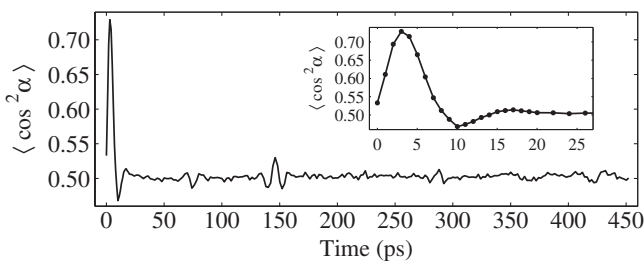


FIG. 3. Alignment dynamics of the molecular plane, represented by $\langle \cos^2 \alpha \rangle$, as a function of time after the short pulse. The laser intensities are as in Fig. 2. The inset is a magnified portions of the early times.

them as half revivals. These arguments are substantiated by theoretical analysis below.

Figure 4 generalizes the experimental results and illustrates their physical origin through quantum mechanical simulations. Numerically, 1D alignment of the C-I axis is quantified by $\langle \cos^2 \theta \rangle$ and $\langle \cos^2 \phi \rangle$ [Fig. 4(a) and 4(c)], where θ is the polar Euler angle between the space-fixed z axis and the molecular C-I axis, and ϕ is the azimuthal angle of rotation of the C-I axis about the space-fixed z axis (i.e., in the plane spanned by the two polarization axes), see Fig. 1(d). For $t < 0$, $\langle \cos^2 \theta \rangle = 0.06$ and $\langle \cos^2 \phi \rangle = 0.93$, illustrating sharp 1D alignment of the molecular C-I axis along the long pulse polarization axis (the idealized limit of perfect 1D alignment corresponds to $\langle \cos^2 \theta \rangle = 0$, $\langle \cos^2 \phi \rangle = 1$). For $t > 0$, $\langle \cos^2 \theta \rangle$ increases to 0.10 and $\langle \cos^2 \phi \rangle$ decreases to 0.87, illustrating a minor distortion of the initial 1D alignment due to the orthogonal short pulse. This evolution agrees well with the experimental information extracted from the I^+ images (Fig. 2).

Rotation about the C-I axis is rigorously described by $\langle \cos^2 \chi \rangle$, χ being the azimuthal Euler angle of rotation about the molecular Z axis (the C-I axis). Our numerical results, Fig. 4(b), illustrate sharp 3D alignment shortly after the short pulse with $\langle \cos^2 \chi \rangle(t = 5 \text{ ps}) = 0.735$. The 3D alignment is followed by a series of partial revivals at a period of ca. $1/(4A)$, corresponding to periodic reconstruction of the 3D alignment with, however, much reduced amplitude as compared to the initial peak. These results agree with the experimental $\langle \cos^2 \alpha \rangle$ values (Fig. 3), illustrating that α makes a good approximation to the angle of rotation about the C-I axis.

Figures 4(d)–4(f) complement Figs. 4(a)–4(c), respectively, and illustrate the origin of the observed effects. At $t < 0$, we find that the sharp 1D alignment induced by the long pulse results from the population of a broad superposition of rotational (J) levels [Fig. 4(d)], where the projection, K , of the total angular momentum, J , on the molecular C-I axis is small [Fig. 4(e)], due to the low rotational temperature offered by our experimental technique. Figure 4(f) illustrates that the C-I axis alignment induced by the long pulse is associated with alignment of the angular momentum vector with a substantial component along the laboratory-fixed z axis. The $t > 0$ portion of panels [Fig. 4(d)–4(f)] illustrate that the short pulse enhances the rotational excitation [Fig. 4(d)] while tilting the J vector with respect to the molecular frame [Fig. 4(e)]. Figure 4(f) illustrates that the orientation of the angular momentum vector with respect to the laboratory frame is only transiently modified by the short pulse, complementing Figs. 4(a) and 4(c). The correspondence of the experimental and numerical results illustrates that the experimental observables, although molecule and probe dependent, reflect directly the 3D alignment and coherent spinning of the molecules and substantiates our confidence in the interpretation of the results.

A variety of avenues for future extensions of this work can be envisioned. First, it may be possible to improve the

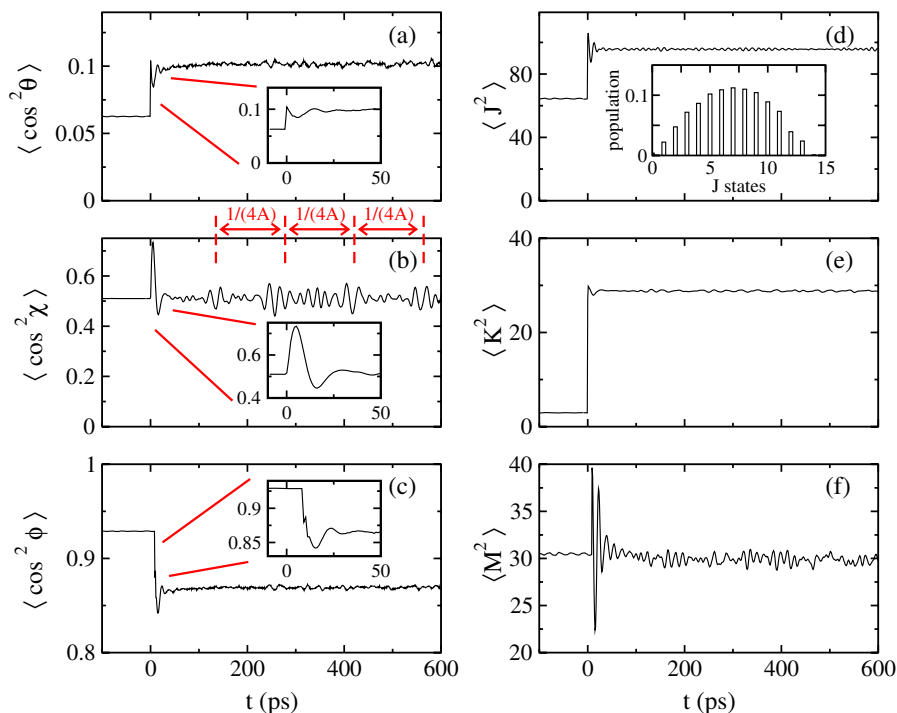


FIG. 4 (color online). Numerical analysis of alignment by a long and a short pulse. $I_{\text{long}} = 1.5 \times 10^{11} \text{ W/cm}^2$, $I_{\text{short}} = 5 \times 10^{12} \text{ W/cm}^2$, $\tau_{\text{short}} = 150 \text{ fs}$, and $T_{\text{rot}} = 0.2 \text{ K}$. (a), (c) Alignment of the C-I axis to the long pulse polarization direction, quantified by $\langle \cos^2 \theta \rangle$ and $\langle \cos^2 \phi \rangle$, (b) alignment of the molecular plane to the plane of the two polarization vectors and subsequent revolution about the C-I axis, quantified by $\langle \cos^2 \chi \rangle$. (d)–(f) The degrees of J , K , and M excitation, respectively. The insets in panels (a), (b), and (c) magnify the short time dynamics, where the center of the short pulse defines the origin of time. The inset in panel (d) illustrates the distribution of the rotational states coherently excited by the long pulse. The arrows in panel (b) point to the periodic interval of $1/4A$ between revivals, illustrating rotation of the molecular plane about the C-I axis.

3D alignment by applying two (or more) optimally timed short pulses. Second, our calculations show that it should be possible to obtain field-free 3D alignment by rapidly truncating the long pulse [19] at the time of the early (and strong) alignment maximum. This method may lead to more efficient field-free 3D alignment compared to a recent scheme based on two short orthogonally polarized pulses [20] because the long pulse produces much stronger 1D alignment than a single short pulse and thus ensures that the 1D alignment is not significantly distorted by the (second) short pulse. Finally, our ability to hold a molecule with a laser pulse and coherently spin it by a second pulse offers new opportunities of studying and controlling the torsion of flexible molecules [21].

Supported by US Department of Energy, the Carlsberg Foundation, the Lundbeck Foundation, and the Danish Natural Science Research Council. This research used resources of the National Energy Research Scientific Computing Center, which is supported by the Office of Science of the US Department of Energy.

- [1] Special issue on Stereodynamics of Chemical Reactions, edited by H.J. Loesch [J. Phys. Chem. A, Vol. 101 (1997)].
- [2] D. Herschbach, Eur. Phys. J. D **38**, 3 (2006).
- [3] B. Friedrich and D. Herschbach, Phys. Rev. Lett. **74**, 4623 (1995).
- [4] T. Seideman, J. Chem. Phys. **103**, 7887 (1995).
- [5] T. Seideman and E. Hamilton, Adv. At. Mol. Opt. Phys. **52**, 289 (2006).
- [6] H. Stapelfeldt and T. Seideman, Rev. Mod. Phys. **75**, 543 (2003).

- [7] J.C.H. Spence and R.B. Doak, Phys. Rev. Lett. **92**, 198102 (2004).
- [8] J. Itatani, J. Levesque, D. Zeidler, H. Niikura, H. Pépin, J.C. Kieffer, P.B. Corkum, and D.M. Villeneuve, Nature (London) **432**, 867 (2004).
- [9] N. Wagner, A. Wuest, I. Christov, T. Popmintchev, X. Zhou, M. Murnane, and H. Kapteyn, Proc. Natl. Acad. Sci. U.S.A. **103**, 13 279 (2006).
- [10] T. Kanai, S. Minemoto, and H. Sakai, Nature (London) **435**, 470 (2005).
- [11] C. Vozzi *et al.*, Phys. Rev. Lett. **95**, 153902 (2005).
- [12] O. Gessner *et al.*, Science **311**, 219 (2006).
- [13] V. Bingelyte, J. Leach, J. Courtial, and M. J. Padgett, Appl. Phys. Lett. **82**, 829 (2003).
- [14] M.D. Poulsen, T. Ejdrup, H. Stapelfeldt, E. Hamilton, and T. Seideman, Phys. Rev. A **73**, 033405 (2006).
- [15] V. Kumarappan, C.Z. Bisgaard, S.S. Viftrup, L. Holme-gaard, and H. Stapelfeldt, J. Chem. Phys. **125**, 194309 (2006).
- [16] This can be seen by noting that the elliptical image is much more radially confined than an image recorded for randomly oriented molecules. In addition, if the C-I axis was strongly misaligned, the I^+ side view at 3 ps would not be as confined as is the case—Fig. 2 (A4).
- [17] J.J. Larsen, K. Hald, N. Bjerre, H. Stapelfeldt, and T. Seideman, Phys. Rev. Lett. **85**, 2470 (2000).
- [18] P.M. Felker, J. Chem. Phys. **96**, 7844 (1992).
- [19] J.G. Underwood, M. Spanner, M.Y. Ivanov, J. Mot-terhead, B.J. Sussman, and A. Stolow, Phys. Rev. Lett. **90**, 223001 (2003).
- [20] K.F. Lee, D.M. Villeneuve, P.B. Corkum, A. Stolow, and J.G. Underwood, Phys. Rev. Lett. **97**, 173001 (2006).
- [21] S. Ramakrishna and T. Seideman, Phys. Rev. Lett. **99**, 103001 (2007).